Heliyon 10 (2024) e32626

Contents lists available at ScienceDirect

Heliyon

journal homepage: www.cell.com/heliyon

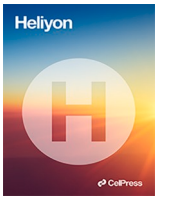

Research article

Mitochondrial dysfunction significantly contributes to the sensitivity of tumor cells to anoikis and their metastatic potential

G.I. Solyanik , D.L. Kolesnik , I.V. Prokhorova *, O.V. Yurchenko , O.N. Pyaskovskaya

Laboratory of Molecular and Cellular Mechanisms of Metastasis, RE Kavetsky Institute of Experimental Pathology, Oncology and Radiobiology, The National Academy of Sciences of Ukraine, Kyiv, 03022, Ukraine

A R T I C L E I N F O

Keywords:
Metastatic potential
Anchorage-independent growth
Mitochondrial dysfunction

A B S T R A C T

It is well-known that the survival of metastatic cells during their dissemination plays an important role in metastasis. However, does this mean that the final result of the metastatic cascade (the volume of metastatic damage to distant organs and tissues) depends on, or at least correlates with, the degree of resistance to anoikis (distinctive hallmarks of metastatic cells)? This question remains open.

The aim of the work was to study *in vitro* the changes in the survival rates, proliferative activity, oxidative stress, and glycolysis intensity during three days of anchorage-dependent and anchorage-independent growth of two Lewis lung carcinoma cell lines (LLC and LLC/R9) and compare these changes with the status of mitochondria and metastatic potential of the cells *in vivo*.

Methods: The number and volume of lung metastases were estimated for each cell line after intramuscular inoculation of the cells in C57Bl/6 mice. For the *in vitro* study, the cells were seeded on Petri dishes pretreated with poly-HEMA or untreated dishes and then allowed to grow for 3 days. Cell viability, cell cycle progression, the level of reactive oxygen species (ROS), glucose consumption and lactate production rates were investigated daily in both growth conditions. An electron microscopy study of intracellular structures was carried out.

Results: The study showed (as far as we know for the first time) a correlation between the metastatic potential of cells (determined *in vivo*) and their sensitivity to anoikis (assessed *in vitro*). The transition of LLC/R9 cells with an inherently defective mitochondrial system to the conditions of anchorage-independent growth was characterized by a decrease in survival, a slowdown in growth rates, an increase in both glucose consumption rate and intracellular ROS levels and manyfold lower metastatic potential, compared to highly metastatic LLC cells with the normal mitochondrial system.

1. Introduction

Despite the extensive progress and successful integration of novel and efficient anticancer medications into oncological practice, metastasis continues to be a major contributor to cancer-related mortality, causing over 90 % of lethal outcomes [1]. Numerous studies concerning the biology of primary tumor growth have led to extensive progress in the creation of effective pharmacological agents that inhibit this process. However, among the large number of drugs used in clinical oncological practice, there is a limited number of

* Corresponding author.
E-mail address: oncom@online.ua (I.V. Prokhorova).

https://doi.org/10.1016/j.heliyon.2024.e32626
Received 19 November 2023; Received in revised form 6 June 2024; Accepted 6 June 2024
Available online 6 June 2024

anticancer agents with a pronounced and effective antimetastatic effect, which is due to a significant lag in understanding the mechanisms of metastasis. One of the main reasons for this lag is the intricate and ever-evolving nature of the metastatic process, which spans the entirety of the body, commencing with the primary tumor and culminating in metastatic sites in distant organs and tissues [2].

It's important to emphasize that anticancer drugs with substantial antimetastatic effect are directed on the suppression of the growth of metastatic lesions [3,4]. These drugs predominantly target the final stage of the metastatic process, diminishing the extent of metastatic damage to normal organs while not affecting the number of metastases. To enhance the effectiveness of cancer therapy, a more promising approach is an exploration of substances capable of impeding the development of the early stages of the metastatic cascade, particularly those influencing the initiation of cancer cell dissemination [5].

It is known that the detachment of normal and malignant cells (of epithelial origin) from the extracellular matrix (ECM) of the tissue generates numerous stress factors, including the loss of growth stimuli from the ECM, the influence of mechanical forces, reorganization of the cytoskeleton, changes in the absorption of nutrients and an increase in the intracellular level of reactive oxygen species (ROS) [6]. In normal and malignant non-metastatic cells, such stress factors induce their apoptotic death (anoikis) [7]. However, most metastatic tumor cells are resistant to anoikis [8], which determines their ability to survive during the circulation in the bloodstream, thereby contributing to the successful colonization of the organism [8,9].

In addition to such factors as growth proteins, pH, transcriptional signaling pathways, which may influence resistance to anoikis and thereby enhance the survival of cancer cells after their detachment (which leads to the oxidative stress [10]), recent studies have identified a key contribution of metabolic pathways that allow cells to bypass anoikis [11,12]. One of the most distinctive hallmarks of cancer cells (compared to normal cells) is the upregulation of glycolysis even in the presence of sufficient oxygen supply. This metabolic phenotype is known as the Warburg effect [13,14]. Despite the well-known fact that such altered glucose metabolism promotes the conversion of glucose into biomass and correlates with the highly proliferative nature of cancer, the glucose requirement of cancer cells during anchorage-independent growth is still poorly understood and remains not characterized [15,16].

There is no doubt that the survival of metastatic cells during their dissemination plays an important role in the process of metastasis. However, does this mean that the final result of the metastatic cascade (the volume of metastatic damage to distant organs and tissues) depends on, or at least correlates with, the degree of resistance of metastatic cells to anoikis? This question remains practically open. Meanwhile, such a correlation (in case it would be revealed) gives grounds to consider the processes that ensure the survival of metastatic cells when they detach from the extracellular matrix as promising targets for antimetastatic therapy.

Here, using two cell lines of Lewis lung carcinoma (LLC and LLC/R9), we have studied *in vitro* the changes in survival rates, proliferative activity, oxidative stress, and glycolysis intensity in these cells during three days of anchorage-independent and anchorage-dependent growth and compared these changes with the status of mitochondria and metastatic potential of them determined *in vivo* by the number and volume of lung metastases.

2. Materials and methods

2.1. Reagents

In the study, the following reagents were used: RPMI 1640 incubation medium (Sigma-Aldrich, USA), fetal calf serum (Biowest, France), poly(2-hydroxyethyl methacrylic) acid (poly-HEMA, Sigma-Aldrich, USA), 2,7-dichlorofluorescein diacetate (Sigma-Aldrich, USA), propidium iodide (Sigma-Aldrich, USA), RNase A (Sigma-Aldrich, USA), trypan blue (Sigma-Aldrich, USA), crystal violet (Sigma-Aldrich, USA), trypsin-Versen solution (Biowest, France), osmium tetraoxide (Sigma, USA), oxamate (Sigma-Aldrich, USA).

2.2. Cell culture

Investigations were carried out using two variants of Lewis lung carcinoma cells (LLC and LLC/R9), obtained from the National Bank of Cell Lines and Tumor Strains of the R.E. Kavetsky Institute of Experimental Pathology, Oncology and Radiobiology of the National Academy of Sciences of Ukraine (IEPOR NASU). Despite the fact that these cell lines have the same genesis, they are characterized by different metastatic potential. Lewis lung carcinoma is a metastatic murine lung cancer model with non-small cell lung cancer histology and high refractory to anticancer therapy.

For both *in vivo* and *in vitro* studies, LLC and LLC/R9 cells were maintained *in vitro* at 37 °C in a humidified atmosphere with 5 % CO_2 in RPMI 1640 incubation medium containing 10 % fetal calf serum (FCS), 40 μg/ml gentamicin and 2 mM L-glutamine.

2.3. In vivo study design

For *in vivo* study, we have used two-month-old female C57Bl/6 mice weighing 19–23 g, bred in the vivarium of the IEPOR NASU. All studies were performed in accordance with the requirements of the Regional Committee for the Ethics of Work with Experimental Animals and in compliance with the rules of work with laboratory animals. 1.0×10^6 LLC or LLC/R9 cells in 0.1 ml of Hanks' solution were inoculated intramuscularly in the thigh of the hind paw of C57Bl/6 mice (9 mice per group).

During the growth of the primary tumor its diameter (D) was measured using a caliper and its volume was calculated by the formula:

$$V_{tum} = 0.52 \bullet D^3$$

After the euthanasia of animals under light ether anesthesia on the 24th day (for LLC) and 23rd day (for LLC/R9) of tumor growth, a macroscopic examination of each animal was carried out, and the size of the primary tumors was recorded. The lungs were removed and the number of metastases in the lungs and their diameter were assessed using a binocular magnifying glass and a millimeter ruler. The volume of lung metastases (Vmet) was calculated accounting their number and size by the formula [17]:

$$V_{met} = \sum \left(n_i \times \frac{3.14 \times d_i^3}{6} \right); \quad d_i = 0.5; \quad 1.0; \quad 1.5; \quad \ldots;$$

where n_i – number of metastases with diameter d_i (mm).

2.4. Histological study

Histological examination of tumor tissue and lung tissue was carried out in at least 5 animals with LLC and LLC/R9 tumors. The material was fixed in a 10 % solution of buffered formalin for 24 h, dehydrated in alcohols of increasing concentrations, starting with 50 % alcohol, embedded in paraffin at a temperature of 56 °C, and then histological sections 5 μm thick were prepared. The resulting sections were stained with hematoxylin-eosin. Analysis of histological sections and subsequent photography of micro slides were carried out using an Axio Star Plus Zeiss microscope.

2.5. In vitro study design

LLC and LLC/R9 cells (0.3×10^6) were seeded in 60 mm Petri dishes. The dishes were either pretreated with poly-HEMA solution [18] to simulate deadhesive growth or left untreated to simulate adhesive cell growth. Coating culture dishes with poly-HEMA inhibits tumor cell adhesion, allowing anchorage-independent cell growth. The cells were incubated for 3 days without changing the incubation medium, which made it possible to study both the kinetics of cell growth and the dynamics of glucose consumption and lactate production rates. The starting cell seeding density (0.3×10^6 cells/dish) ensured non-confluent cell growth and sufficient cell numbers for research within 3 days. Cell count, viability, apoptotic cell number, cell cycle phase distribution, intracellular ROS levels, glucose and lactate concentrations in the incubation medium were evaluated daily for 3 days of cell growth. The study was performed primarily in quadruplicate for each growth time period, cell line, and growth conditions.

2.6. Cell viability assay

The number of cells and their viability were evaluated by a routine method using direct cell counting in a hemocytometer using a 0.4 % trypan blue solution.

2.7. Cell cycle progression

The distribution of cells by cell cycle phases and the number of apoptotic cells were determined using flow cytofluorometry [19]. For this, cells were resuspended in a hypotonic lysis buffer with the addition of propidium iodide and RNase A, and the DNA content was analyzed on a FACSCalibur flow cytometer (Becton Dickinson, USA) with a 488 nm argon laser and a 582/42 nm filter. Flow cytofluorometry data were analyzed using the ModFit LT 3.0 program (BDIS, USA). The level of apoptosis was assessed by the number of cells with hypodiploid DNA content which reflected huge cell DNA fragmentation in the late stage of apoptosis.

2.8. Reactive oxygen species (ROS) levels

The level of intracellular ROS in cancer cells was determined using 2,7-dichlorofluorescein diacetate using flow cytofluorometry [20]. Briefly, cells were washed twice with phosphate-buffered saline (pH 7.4) and incubated in RPMI 1640 medium without FCS with the addition of 2,7-dichlorofluorescein diacetate at 37 °C for 30 min. After that, cells were washed twice with phosphate-buffered saline and analyzed on a FACSCalibur flow cytometer (Becton Dickinson, USA) with a 488 nm argon laser and a 530/30 nm filter. For each sample, 20,000 events were analyzed, while the percentage of cell staining was about 100 % (99.60–99.95 %). To determine the autofluorescence background rate, non-stained LLC cells were used. The GeoMean score calculated by the flow cytometer software was used as the value of intracellular ROS level per single cell.

2.9. Determination of the glucose consumption and lactate production rates

Determination of glucose and lactate concentrations in the incubation medium of cancer cells was conducted using a ChemWell 2910 biochemical analyzer (Awareness Technology, USA) with commercial kits designed for glucose determination employing glucose oxidase (Global Biomarketing Group, Inc, USA), and lactate determination utilizing lactate oxidase (Global Biomarketing Group, Inc, USA), following the manufacturer's instructions.

The glucose consumption rate (GCR, expressed in 10^{-9} mmol/cell/day) was computed utilizing the following formula:

$$GCR = 2 \times \frac{\left(C_{gl}(t_i) - C_{gl}(t_{i+1})\right) \times V}{N(t_i) + N(t_{i+1})}$$

where $C_{gl}(t_i)$ *and* $C_{gl}(t_{i+1})$ are the concentrations of glucose in the incubation medium at t_i and t_{i+1} – two consecutive days of cell growth, $N(t_i)$ *and* $N(t_{i+1})$ are the counts of cells on corresponding consecutive days of growth; V is the volume of the incubation medium which in the study was equal to 6×10^{-3} L [21].

The lactate production rate (LPR, expressed in 10^{-9} mmol/cell/day) was calculated by the following formula:

$$LPR = 2 \times \frac{(C_l(t_{i+1}) - C_l(t_i)) \times V}{N(t_i) + N(t_{i+1})}$$

where $C_l(t_i)$ *and* $C_l(t_{i+1})$ are the concentrations of lactate in the incubation medium at t_i and t_{i+1} – two consecutive days of cell growth, $N(t_i)$ *and* $N(t_{i+1})$ are the counts of cells on corresponding consecutive days of growth; V is the volume of the incubation medium which in the studies was equal to 6×10^{-3} L.

2.10. Electron microscopy study

For an electron microscopy study LLC and LLC/R9 cells after one day of adhesive growth were quickly washed with PBS, mechanically removed and centrifuged for 5 min at 1500 rpm. After that the cells were fixed with a 2.5 % solution of glutaraldehyde in 0.1 M cacodylic acid buffer (pH = 7.4) for 1 h at 4 °C [22]. 2 % solution of osmium tetroxide in 0.1 M sodium cacodylate buffer was used to complete cell fixation. After that the cells were dehydrated (in a graded series of ethanol/acetone) and polymerized in an Epon–Araldite epoxy resin mixture. Sections were obtained using an ultramicrotome and stained with 0.2 % solution of uranyl acetate and Reynold's solution (lead acetate). The stained sections were studied using a JEM100B electron microscope at an accelerating voltage of 60 kV.

2.11. Cytological study

LLC and LLC/R9 cells, after adhesive and deadhesive growth for 3 days, were transferred to coverslips and incubated in a standard incubation medium for 4 h in order to attach the cells to the surface of the slides. After 4 h, slides with cells were washed with PBS and sequentially stained according to Romanovsky [23]. Then the slides were washed with distilled water, dried in air and sealed in glycerin. Cytological studies were performed using an AxioStar Plus Zeiss optical microscope (Germany). For each cell line, 100 cells were analyzed in different fields of view of the cytological preparation, counting the number of rounded, elongated and elongated multinucleated cells. For each cytological preparation, at least 10 fields of view located in different areas of the preparation, were analyzed. The observed results were recorded using a Canon PowerShot G5 digital camera at × 400 magnification.

2.12. Statistical analysis

The statistical analysis encompassed descriptive statistics, Student's t-test, Mann-Whitney U test. The data is presented as M±SE, where M represents the mean value, and SE is the standard error. The differences were considered statistically significant if $p < 0.05$.

3. Results

3.1. In vivo study of LLC and LLC/R9 growth and metastasis

In vivo study showed no significant differences in the volume of the primary tumors between the two variants of Lewis lung carcinoma at the end of the experiment (Table 1). It should be noted that the analysis of growth kinetics showed that in the exponential growth phase (between 12 and 18 days) the growth rate of LLC/R9 was higher compared to LLC. However, at later stages, a slowdown in the growth rate of this LLC/R9 variant was observed (Fig. 1).

Despite the lack of differences in the growth kinetics of LLC and LLC/R9, these cell lines were shown to differ significantly in their metastatic potential. Thus, the number of metastases in the lungs of mice with LLC/R9 was 4 times lower ($p < 0.002$), and their volume was more than 10 times lower ($p < 0.004$) compared to these indicators in animals with LLC (Table 1).

Table 1
Tumor volume, number, and volume of lung metastases on 24 days (for LLC) and 23 days (for LLC/R9) of tumor growth.

Cell type	Tumor volume (mm^3)	Number of lung metastases	Volume of lung metastases (mm^3)
LLC	683.4 ± 76.5	32.3 ± 5.3	67.3 ± 14.6
LLC/R9	745.4 ± 62.3	8.0 ± 1.3*	6.3 ± 1.0*

Note: The differences are significant ($p < 0.005$) compared to the corresponding values for LLC.

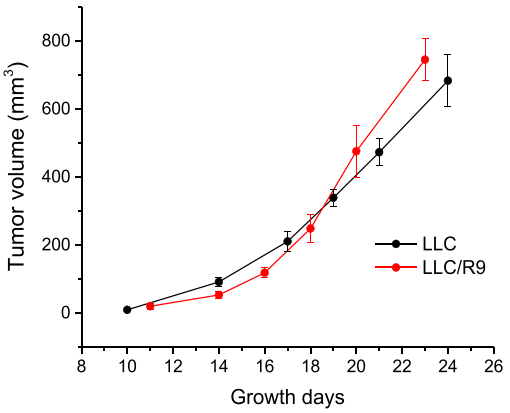

Fig. 1. Growth kinetics of LLC and LLC/R9 cells.

3.2. The histological study

The histological structure of the LLC/R9 tumor (Fig. 2b) showed some peculiarities that differ this tumor from the LLC strain (Fig. 2a). First of all, this is related to the polymorphism of tumor cells, which was not observed when studying the morphology of the LLC tumor. The LLC/R9 tumor was composed from small, medium, and large cells with a predominance of the latter. Another distinctive feature of the histological structure of LLC/R9 was the appearance of a large number of vessels, often much bigger compared to LLC (Fig. 3a). Red blood cells accumulated in some vessels and hyalinosis were also observed. It should be noted that the phagocytic activity of LLC/R9 tumor cells was more pronounced (compared to LLC), as a result of which light-optical empty areas with small remnants of dead cells were recorded in the tumor tissue (Fig. 3b).

3.3. Cell proliferation

Survival of LLC and LLC/R9 cells during 3 days of anchorage-independent growth was evaluated and compared with the cells under adherent growth conditions for the same time period.

During the growth of both LLC and LLC/R9 cells on a deadhesive substrate, a notable reduction in the growth rate was observed in comparison to the adhesive growth type. This slowdown was most evident on the 3rd day (Fig. 4). Specifically, the number of viable cells in both cases (LLC and LLC/R9) on the 3rd day of deadhesive growth was significantly lower by 33.5 % ($p < 0.05$) and 37.6 % ($p < 0.05$), respectively, compared to the adhesive growth conditions. At the same time, the number of viable LLC/R9 cells in both adhesive and deadhesive growth conditions was by 20 % and 25 % ($p < 0.05$) lower than these indices for LLC cells.

3.4. Glucose consumption, lactate production

The growth of both cell lines during three days was accompanied by the changes in glucose consumption and lactate production. For LLC cells, a progressive decrease in the level of glucose in the incubation medium and an increase in the level of lactate were equally pronounced in both adhesive and deadhesive growth conditions (Fig. 5). In contrast to LLC, LLC/R9 cells showed a relatively small but significant increase in glucose levels in the incubation medium by 13 % ($p < 0.05$) and a decrease in lactate levels by 10 % ($p < 0.05$) on the 3rd day compared with the corresponding values during adhesive growth.

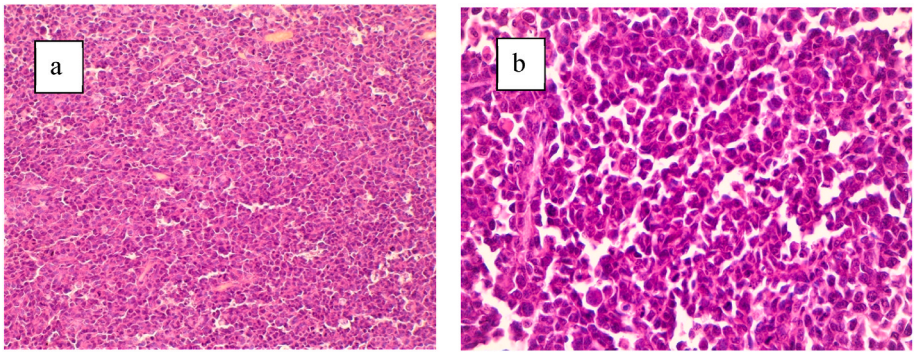

Fig. 2. Pronounced polymorphism of LLC/R9 cells (b; the amount of magnification is 400) compared to LLC cells (a, the amount of magnification is 200).

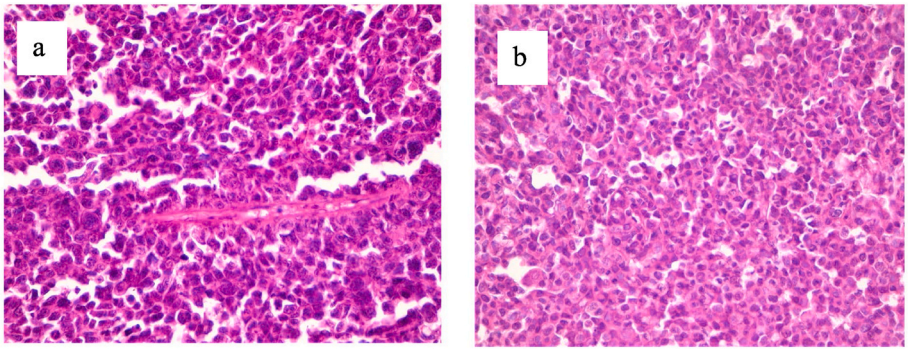

Fig. 3. Blood vessel (a) and manifestations of phagocytic activity (b) in LLC/R9 tumor (the amount of magnification is 400).

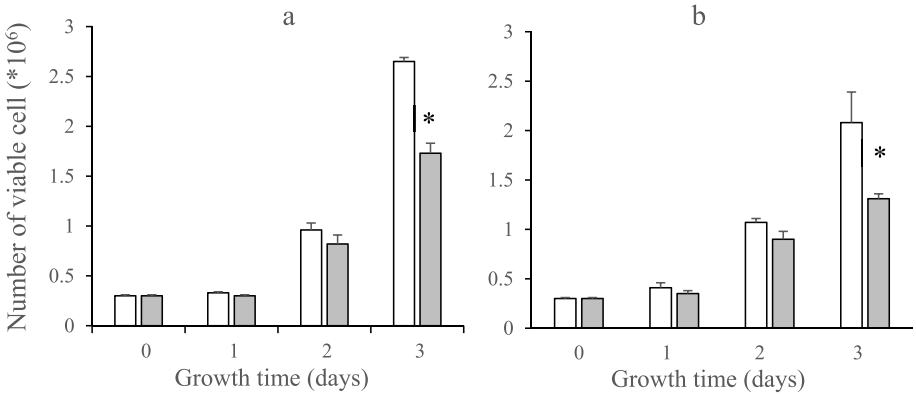

Fig. 4. Growth kinetics of LLC (a) and LLC/R9 (b) cells during adhesive (white columns) and deadhesive (gray columns) growth. Note: * – the significant difference compared to the corresponding indices for adhesive growth conditions (p<0.05).

The absence of significant differences (in the case of LLC) or minor differences (in the case of LLC/R9) in the level of glucose in the incubation medium during cell growth on a deadhesive substrate (when a progressive decrease in the number of viable cells was recorded compared to adhesive conditions) indicates a possible increase in the rate of glucose uptake by LLC cells and LLC/R9 during anchorage-independent growth, which is confirmed by the results of the corresponding calculations.

The rates of both glucose consumption and lactate production (Tables 2 and 3) by LLC cells during three days of deadhesive growth practically did not change. However, due to the progressive decrease in the glucose consumption rate during the adhesive growth of these cells, the value of this indicator on the 2nd and 3rd days of deadhesive growth was significantly higher than during adhesive growth, by 56.4 % and 37.1 % (on the 2nd and 3rd days, respectively).

In contrast to LLC cells, LLC/R9 cells exhibit an increase in glucose consumption during both adhesive and deadhesive growth. Thus, on the 3rd day of growth, the glucose consumption rates significantly increased by 65.8 % (in adhesive growth conditions) and by 54.3 % (in conditions of deadhesive growth) compared to the 1st day. However, despite a significant increase in glucose consumption rates by these cells, the rate of lactate production for three days did not change during the growth in both conditions.

3.5. Cell cycle progression

During three days of adhesive growth of LLC cells, the research has revealed minor variations in the distribution of cells by cell cycle phases. Notably, there was a trend indicating a decrease in the number of cells in the S phase and an increase in the number of cells in the G2/M phase on the 2nd day of growth (Fig. 6).

Another pattern of proliferative heterogeneity was observed when these cells were grown on a deadhesive substrate. Following 1 day of growth of LLC cells, a notable 2-fold increase in the number of cells in the S phase ($p < 0.05$) was observed, primarily attributed to a reduction in the number of cells in the G1/0 phase (by 41 %, $p < 0.05$) and the G2/M phase (by 67.7 %, $p < 0.05$) of the cell cycle. This pattern persisted on the 2nd day of growth, although the differences in the number of cells in the $G_{1/0}$, S, and G_2/M phases of the cell cycle during deadhesive growth (compared to the adhesive) were somewhat lower (however, they were statistically significant). Three days later, the proliferative activity of LLC cells during deadhesive growth decreased to the corresponding values of adhesive growth. Consequently, the proliferative heterogeneity among LLC cells after three days of anchorage-independent growth remained comparable to that observed in anchorage-dependent conditions.

In contrast to LLC cells, during the growth of LLC/R9 cells under both adhesive and deadhesive conditions, the distribution of cells

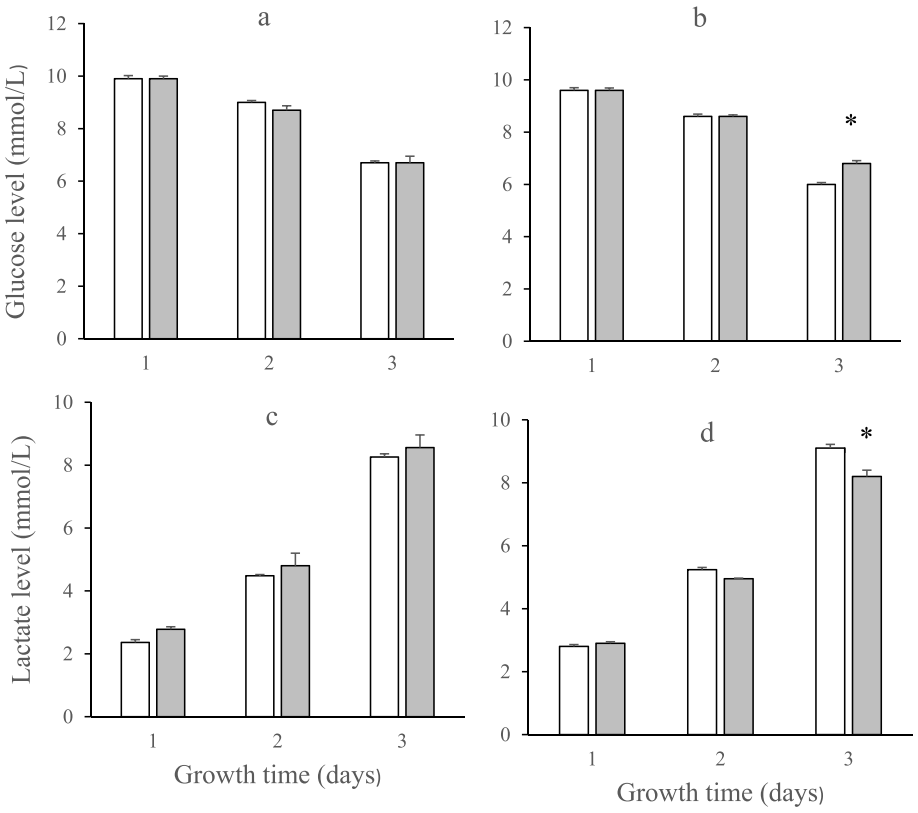

Fig. 5. Glucose (a, b) and lactate (c, d) levels in incubation medium during adhesive (white columns) and deadhesive (gray columns) growth of LLC (a, c) and LLC/R9 (b, d) cells. Note: * – differences are statistically significant compared to the corresponding value for adhesive growth ($p < 0.05$).

Table 2
The glucose consumption rate of both LLC and LLC/R9 cells during adhesive and deadhesive growth.

Growth type	Glucose consumption rate (10^{-9} mmol/cell/day)		
	1st day	2nd day	3rd day
LLC			
Adhesion	15.2 ± 0.7	11.25 ±0.9[1]	10.5 ±0.4[b]
Deadhesion	16.3 ± 0.9	17.6 ± 2.1[a]	14.4 ± 1.1[a]
LLC/R9			
Adhesion	12.0 ± 1.4	15.4 ± 1.6	19.9 ±2.3[b]
Deadhesion	12.7 ± 1.3	18.3 ±1.9[b]	19.6 ±2.0[b]

Note.
[a] The significant difference compared to the corresponding indices during adhesive growth conditions ($p<0.05$).
[b] The significant difference compared to the 1st day of the corresponding growth conditions ($p<0.05$).

Table 3
The lactate production rate of both LLC and LLC/R9 cells during adhesive and deadhesive growth.

Growth type	Lactate production rate (10^{-9} mmol/cell/day)		
	1st day	2nd day	3rd day
LLC			
Adhesion	13.5 ± 0.7	19.7 ±1.6[b]	12.7 ± 1.4
Deadhesion	22.4 ± 1.1[a]	20.9 ± 2.3	18.2 ± 2.0[a]
LLC/R9			
Adhesion	16.9 ± 1.9	19.5 ± 2.0	14.9 ± 2.1
Deadhesion	20.3 ± 1.6	20.2 ± 2.0	17.5 ± 1.8

Note.
[a] The significant difference compared to the corresponding indices during adhesive growth ($p<0.05$).
[b] The significant difference compared to the 1st day of the corresponding growth conditions ($p<0.05$).

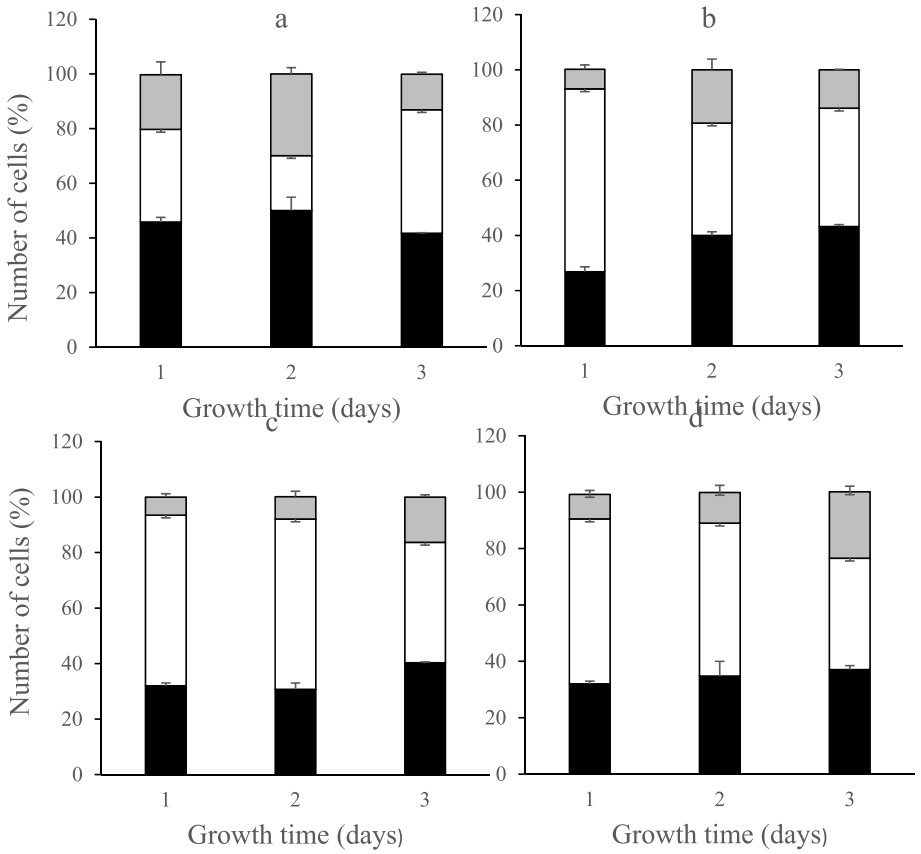

Fig. 6. Changes in cell cycle progression of LLC (a, b) and LLC/R9 (c, d) cells during adhesive (a, c) and deadhesive (b, d) growth. Number of cells (in %) in G_2/M phase (gray), S phase (white) and G_1/G_{10} phase (black).

over the phases of the cell cycle did not change for two days, after which a decrease in their proliferative activity was observed, more pronounced in the case of anchorage-independent growth (Fig. 6). Thus, the number of cells in the S phase after three days of adhesive growth was significantly lower by 29.5 % ($p < 0.05$) and by 32.5 % ($p < 0.05$) after three days of deadhesive growth compared with the corresponding indicators after the 1st day of growth. Such a decrease for both growth types was mainly due to an increase in the number of cells in the G_2/M phase, which was much more pronounced in the case of anchorage-independent growth. Thus, the number of LLC/R9 cells in the G_2/M phase on the 3rd day of deadhesive growth was 44 % ($p < 0.05$) higher compared to that in adhesive growth conditions.

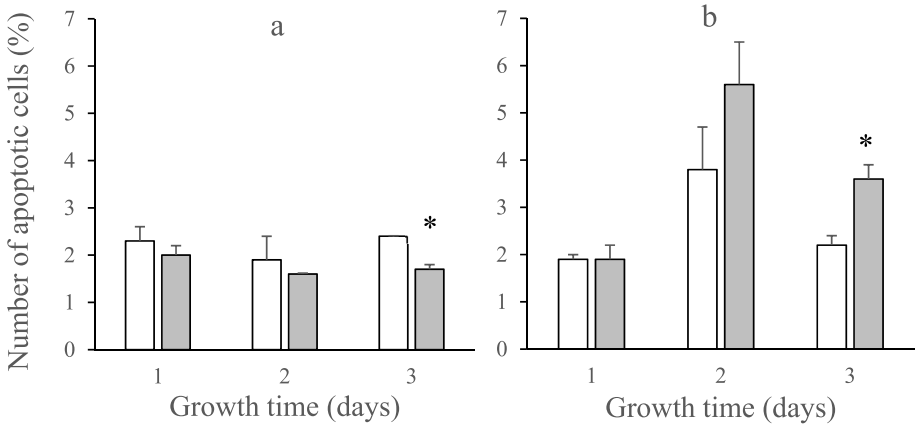

Fig. 7. Changes in the number of apoptotic LLC (a) and LLC/R9 (b) cells during adhesive (white columns) and deadhesive (gray columns) growth. Note: * – the significant difference (p<0.05) compared to the corresponding indices for adhesive growth.

3.6. Apoptosis

It should be noted that both cell lines showed a modest level of apoptotic cell death. However, a comparative analysis of changes in the number of apoptotic cells during cell growth on a deadhesive substrate showed fundamental differences between LLC and LLC/R9 cells (Fig. 7). Hence, the number of apoptotic LLC cells on the 3rd day of anchorage-independent growth exhibited a notable 29 % decrease ($p < 0.05$) in comparison with anchorage-dependent growth. In contrast to LLC, the apoptotic death of detached LLC/R9 cells significantly increased by 63 % ($p < 0.05$) on the 3rd day of growth compared to adherent growth.

3.7. ROS production

As shown in Fig. 8, during the adhesive and deadhesive growth of LLC cells, the intracellular ROS levels progressively decreased, more significantly during the adhesive growth conditions. So, on the 2nd and 3rd days of anchorage-independent growth, the level of ROS was more than 2 times ($p < 0.01$) higher than during anchorage-dependent growth.

The dynamics of changes in the intracellular levels of ROS in LLC/R9 cells differed from LLC during both adhesive and deadhesive growth (Fig. 8). A significant (by 90 %, $p < 0.01$) decrease in the level of ROS was observed only on the 3rd day of anchorage-dependent growth of LLC/R9 cells. During anchorage-independent growth, the ROS level did not change for three days, maintaining its high values. It should be noted that the intracellular level of ROS in LLC/R9 cells was significantly higher by 2–5 times ($p < 0.01$) compared with the corresponding indices of LLC cells during both adhesive and deadhesive growth.

3.8. Electron microscopic study

Electron microscopic examination of LLC and LLC/R9 cells during the 1st day of adhesive growth revealed significant differences between these cells (Fig. 9). Thus, it was revealed that, unlike LLC (Fig. 9a), a significant part of the mitochondria of LLC/R9 cells showed characteristic morphological signs of an inactive state (Fig. 9b). As can be seen in Fig. 9b–a large number of mitochondria in LLC/R9 cells are small, electron-dense, with closely adjacent cristae. Dysfunction of a large part of the mitochondria, found in LLC/R9 cells, may cause low oxidative phosphorylation activity and greater sensitivity of these cells to hypoxia compared to LLC. The percentage of apoptotic cells after a one-day adhesive growth of LLC/R9 cells in conditions of severe hypoxia (<1 % O_2) was 14.8 ± 3.7, which was 4 times higher than the corresponding index in normoxic conditions (3.7 ± 0.5; $p < 0.01$). At the same time, hypoxia practically did not affect the level of apoptotic death of LLC cells (5.9 ± 0.8 % and 7.4 ± 1.3 % under normoxia and hypoxia conditions, respectively).

3.9. Cytological study

A comparative cytological study of LLC and LLC/R9 cells on the 3rd day of adhesive and deadhesive growth was carried out. Cells were incubated for 4 h on coverslips. The study has shown the heterogeneity of the cell populations of both variants manifested in the existence of rounded and elongated cells. Among the latter, there were large cells containing 2–3 nuclei. So, despite the fact that during the deadhesive growth of LLC cells, the number of elongated cells increased by almost 2 times ($p < 0.001$) compared to the adhesive type of growth (due to a significant decrease in the number of rounded mononuclear cells), the number of large multinucleated cells during the deadhesive growth of LLC did not differ from their number during adhesive growth (Table 2, Fig. 10 d,e)

An increase in the number of elongated multinucleated LLC/R9 cells during deadhesive growth (black arrows)

The number of elongated LLC/R9 cells during deadhesive growth also increased almost 2 times ($p < 0.001$) compared to adhesive

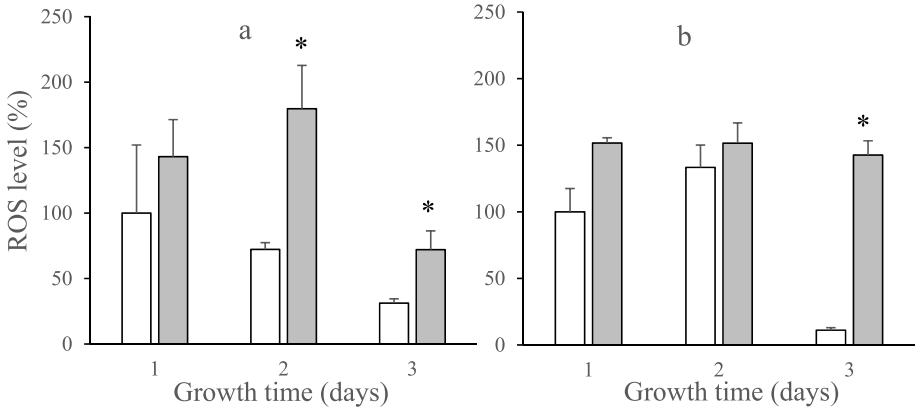

Fig. 8. The intracellular ROS levels in LLC (a) and LLC/R9 (b) cells during adhesive (white column) and deadhesive (gray column) growth (as a percentage of the corresponding ROS levels on the 1st day of adhesive growth). Note: * – the significant difference ($p < 0.01$) compared to the corresponding indices for adhesive growth.

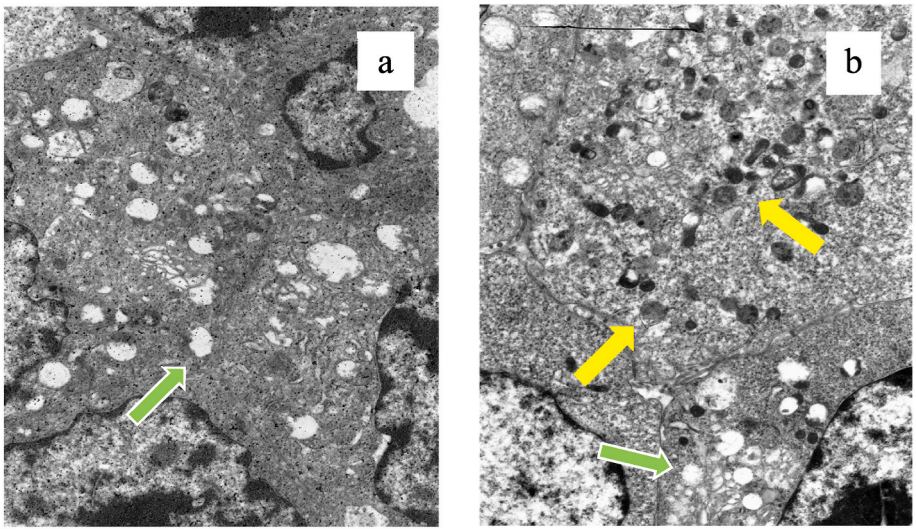

Fig. 9. Electron microscopic study of LLC (a) and LLC/R9 (b) cells during adhesive growth (x10000). Normal mitochondria (green arrows) and optically dense (yellow arrows).

growth. However, in contrast to LLC, the part of large multinucleated cells significantly increased by 117 % ($p < 0.005$), in comparison with the adhesive type of growth (Table 4, Fig. 10a, b,10c).

4. Discussion

Resistance of cancer cells (of epithelial origin) to anoikis is currently considered one of the few known characteristics of metastatic cells that distinguish them from non-metastatic counterparts [24,25]. The ability of metastatic cells to survive after detachment from the extracellular matrix is necessary for the development of the entire metastatic cascade, ensuring their spread throughout the body with blood as the main transport system. Therefore, resistance to anoikis is inherent in all metastatically active cells, regardless of their metastatic potential [26]. But this distinctive characteristic is not enough to enable the cell to survive throughout the entire metastatic cascade with the final formation of secondary tumors in distant organs and tissues. The colonization of distant tissues by disseminated cancer cells is well-known as an extremely inefficient process [27]. While relatively numerous circulating tumor cells (CTCs) are detected in the blood of cancer patients, with reports indicating >1000 CTCs/ml of blood plasma, disproportionally few metastases are clinically detectable [28]. Therefore, the number of metastases and their volume (characteristics that determine the metastatic potential of cancer cells) is determined by the ability of some of the circulating and anoikis-resistant cells to survive at all stages of the metastatic cascade following intravasation.

These features undoubtedly include the metabolic adaptability of metastatic cells. In the process of metastasis, cells encounter a constantly changing metabolic microenvironment, which differs significantly at different stages of the metastatic cascade [29]. This means that in order to form a metastatic node, cancer cells must survive in a spatially heterogeneous and nutrient-deficient microenvironment of the primary tumor, followed by intravasation into the vascular system. The latter requires not only the ability to avoid apoptotic death and oxidative stress under detachment, but also to adapt to a high content of oxygen, glucose, and glutamine in the bloodstream (we leave out the influence of a large number of humoral factors and components of the immune system) [30]. Extravasation to distant organs is accompanied by a significant decrease in the level of nutrient substrates and a high level of humoral factors produced by normal cells of the target organ. Thus, in order to implement the entire metastatic cascade, tumor cells must have a unique metabolic plasticity capable of ensuring their adaptation to constantly changing metabolic conditions [31,32]. This ability to reprogram cellular metabolism has been recognized as one of the necessary distinctive properties of metastatic cells [33,34].

It should be noted that altered metabolism is a universal property of practically all cancer cells. The most significant change in glucose metabolism is manifested in a drastically increased glucose consumption even in the presence of sufficient oxygen and also in a significant weakening of the relationship between glycolysis and the mitochondrial TCA cycle and OXPHOS. In the 1920s Otto Warburg (a pioneer in quantitative investigations of cancer cell metabolism) and co-workers showed that under aerobic conditions tumor tissues metabolize approximately tenfold more glucose to lactate in a given time than normal tissues (a phenomenon known as the Warburg effect.) [35,36]. This feature of the glycolytic metabolism of cancer cells reduces the risk of apoptotic death during matrix detachment (contributing to the resistance of these cells to anoikis and their capability to metastasis) by moderating the high level of ROS generated during glucose oxidation [16,26]. The question arises whether there is a correlation between the metastatic potential of tumor cells, the degree of resistance to anoikis, and the intensity of aerobic glycolysis.

In this regard, firstly we estimated *in vivo* the metastatic potential of two variants of Lewis lung carcinoma cells (LLC and LLC/R9). We showed that these two LLC variants differed significantly in their metastatic potential: LLC cells were highly metastatic and LLC/R9 cells were low metastatic. So, the number of lung metastases in animals with LLC/R9 was 4 times lower, and their volume was more

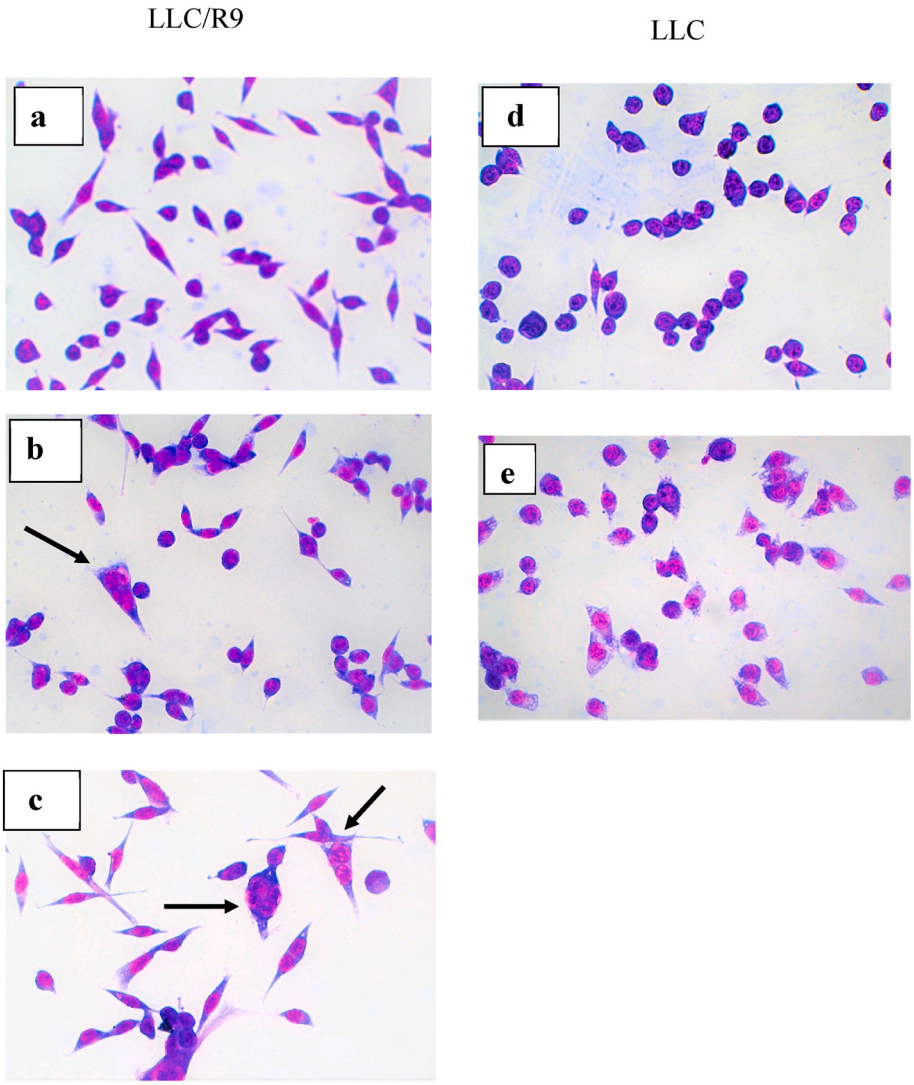

Fig. 10. LLC/R9 (a, b, c) and LLC (d, e) cells after 3 days of adhesive (a – for LLC/R9; d – for LLC) and deadhesive (b, c – for LLC/R9; e – for LLC) growth.

Table 4
The number of elongated (mononuclear and multinucleated) LLC and LLC/R9 cells on the 3rd day of adhesive and deadhesive growth.

Cell type	Growth type	Number of elongated cells (% from total)	Number of multinucleated cells (% from elongated)
LLC	Adhesive	14.2 ± 0.8	1.2 ± 0.3
	Deadhesive	33.4 ± 1.2[a]	1.7 ± 0.2
LLC/R9	Adhesive	37.3 ± 1.9	2.4 ± 0.3
	Deadhesive	70.4 ± 1.5[a]	5.2 ± 0.3[a]

Note.
[a] The significant difference compared to the corresponding indices for adhesive growth conditions (p<0.05).

than 10 times lower as compared to the corresponding parameters of LLC (Table 1).

To find an answer on the mentioned above question, we conducted a comparative *in vitro* study of the changes in the survival, proliferative activity, and glycolysis of LLC and LLC/R9 cells during 3 days of anchorage-dependent and anchorage-independent growth.

Our studies have shown that during three growth days of cells with a high metastatic potential (LLC) on an adhesive substrate, the number of cells increased exponentially, which was accompanied by a progressive decrease in the rate of glucose consumption as well as a decrease in the intracellular level of ROS (Table 2, Fig. 8).

The maintenance of high proliferative activity and control of ROS escalation against the background of a decrease in glucose consumption indicated the possible involvement of glutamine in the metabolism of these cells.

Recent studies have pointed out that, like glycolysis, glutamine metabolism plays an important role in the growth and survival of cancer cells (including lung cancer cells) due to its ability to support biosynthesis of macromolecules and maintain bioenergetics and redox balance of cancer cells [37–39]. Formally, metabolic changes other than the Warburg effect, which undoubtedly include the activation of glutamine metabolism, are probably necessary to reduce oxidative stress that accompanies the entire metastatic cascade [40]. There is a reason to believe that tumor cells with high metastatic potential should exhibit abnormal glucose and glutamine metabolism to confer their growth and survival under both adhesive and deadhesive conditions.

A study of LLC during anchorage-independent growth showed that the growth rate of detached LLC cells was lower compared to the adhesive type of growth so that on the 3rd day the number of detached cells decreased by more than 30 % (Fig. 4) The analysis revealed that such a decrease was not due to cell death (either by necrotic or apoptotic type), but most likely was caused by cell arrest in the S phase of growth, which occurred already on the 1st day of growth and manifested itself, although to a lesser extent and on the 2nd day. So, on the 1st day, a significant increase in the number of deadhesive cells in the S phase was recorded (compared to adhesive growth), despite the fact that there was no increase in their total number (Fig. 6). In the absence of external DNA damaging agents, the question about the mechanisms for such an arrest remained open. A real candidate was ROS (as a DNA damaging endogenous factor), and although the level of ROS after the 1st day of deadhesive growth was quite high, however, due to the significant variability of this indicator on the 1st day of adhesive growth, no significant differences were recorded between them.

In the process of anchorage-independent growth, the intracellular level of ROS progressively decreased, remaining, however, at a much higher levels both on the 2nd and 3rd days compared to adhesive growth. At the same time, in contrast to attached cells, the rate of glucose consumption by detached LLC cells did not change during their growth and was significantly higher on the 2nd and 3rd days compared to the rates of these cells during adhesive growth (Table 2). This indicated a more pronounced involvement of glycolysis in inhibiting the ROS elevation in detached LLC cells compared to attached ones.

Our study has shown that many characteristics of the low-metastatic LLC/R9 cells differed significantly from those of highly metastatic LLC cells under both adhesive and deadhesive growth conditions. In particular, the growth rate of attached LLC/R9 cells was significantly lower than that of LLC cells (Fig. 4). This was largely due to a significant increase in the number of apoptotic cells, especially on the 2nd day of growth (by 100 % compared to the 1st day), while maintaining a fairly high level on the 3rd day (Fig. 7). This correlated with a high intracellular level of ROS, which did not change during two days of growth. Similarly, to ROS, the distribution of cells by cell cycle phases practically did not change during two days of growth. However, on the 3rd day, there was a significant decrease in the number of cells in the S phase (due to a significant increase in the number of cells in the G1/0 and G2/M growth phases) and a significant drop in the ROS levels. The decrease in the level of ROS in LLC/R9 cells, observed on the 3d day of adhesive growth (Fig. 8), correlated with a significant increase (>65 %) in glucose consumption rate without the change in the rate of lactate production.

Significant differences between the cells of LLC/R9 and LLC variants were also observed during deadhesive growth. In particular, during 3 days of growth, the levels of ROS in LLC/R9 cells did not change, maintaining high values (while the dynamics of changes in the intracellular level of ROS in LLC cells was characterized by a progressive decrease during adhesive and deadhesive growth) (Fig. 8). Such oxidative stress caused a high level of apoptotic death of LLC/R9 cells, which on the 3rd day was more than 44 % higher compared to that of attached LLC/R9 cells and more than 2 times higher compared to the level of apoptotic death of both adhesive and deadhesive LLC cells (Fig. 7). Also, the growth of detached LLC/R9 cells was accompanied by a significant increase in the rate of glucose consumption on the 2nd and 3rd days. At the same time, the rate of lactate production did not change during cell growth. This may indicate a redirection of glucose either to the oxidative branch of the pentose phosphate pathway (PPP) (with the formation of NADPH, which is a necessary cofactor for replenishment of the most important cell antioxidant - reduced glutathione) or to an increased glucose oxidation, which, due to the defectiveness of the mitochondrial system of LLC/R9 cells may increase oxidative stress. Regardless of the change in glycolysis, its intensification in deadhesive LLC/R9 cells did not provide the detoxification of ROS.

In contrast to LLC cells, during the growth of detached LLC/R9 cells their distribution by the phases of the cell cycle did not change for two days, after which a decrease in the number of cells in the S phase by more than 30 % was observed due to an increase in the number of cells in the G2/M phase (Fig. 6). This indicated G2/M arrest of LLC/R9 cells, which usually occurred due to DNA damage (in our case due to a very high level of ROS). Interestingly, the arrest of non-attached LLC/R9 cells in the G2/M phase, as well as a high level of ROS on the 3rd day of growth, correlated with the appearance of large multinucleated cells, the number of which was almost 2 times higher compared to their number in attached LLC/R9 cells. (Fig. 9). It should be noted that the mechanism of neoplastic multinucleation remains unknown, but is considered to be induced by either cell-cell fusion or acytokinetic cell division [41]. The latter can be induced by the DNA-damaging action of ROS [42]. Unlike low metastatic LLC/R9 cells, large multinucleated cells among the highly metastatic LLC cells were virtually absent.

Comparative studies have shown that LLC and LLC/R9 differed significantly in both metastatic potential (determined *in vivo*) and indicators of survival, proliferative activity, and intensity of glycolysis during anchorage-independent growth (based on *in vitro* studies). A more pronounced sensitivity to anoikis of low metastatic LLC/R9 cells correlated with high intracellular ROS levels (manyfold higher compared to highly metastatic LLC cells).

It is well known that mitochondria are the most prominent sources of ROS within a cell that contribute to oxidative stress [43]. The intracellular level of ROS is a balance between their generation (mainly as a bypass product during oxidative phosphorylation in mitochondria) and the neutralizing effect of the cell's antioxidant system [44,45]. A high level of ROS in a cell may result from either their active generation or inactivation by an antioxidant system or both. Electron microscopic study of intracellular structures of LLC and LLC/R9 cells during their one-day adhesive growth revealed significant differences between them (Fig. 9). It was shown that, in

contrast to LLC, a significant part of mitochondria in LLC/R9 cells exerted morphological signs of an inactive state: they were small, electron-dense, with closely adjacent cristae. This indicates a defect in the mitochondrial system of LLC/R9 cells, which may be one of the reasons for the observed extremely high level of ROS during anchorage-dependent and anchorage-independent growth.

The discovery of high rates of aerobic glycolysis in cancer cells by Otto Warburg in the late 1920s led him to assume that respiration, through oxidative phosphorylation (OXPHO), is impaired or damaged in all cancer cells [46]. Further studies showed that the high rate of glucose metabolism is maintained in different cancer cells despite the occurrence of OXPHO [47]. Therefore, dysfunction of the mitochondrial system is not a necessary condition that causes the intensification of glucose metabolism.

Meanwhile, disruption of the respiratory branch of cancer cells may be a sufficient condition for increasing the rate of glucose metabolism to control the escalation of ROS production that occurs when there are disturbances in the mitochondrial electron transport system [48,49]. In our study, LLC/R9 cells with an inherently defective mitochondrial system are characterized by a higher rate of glucose uptake (compared to LLC cells with the normal mitochondrial system), from 2- to 5-fold higher intracellular ROS levels, lower survival during anchorage-independent growth and many folds lower metastatic potential.

The results of the study indicated that pharmacological agents capable of activating oxidative phosphorylation can exhibit a pronounced cytotoxic effect against cancer cells with a defective mitochondrial system. Thus, for example, the high selective toxicity of dichloroacetate (a pyruvate mimetic that stimulates oxidative phosphorylation inhibition through pyruvate dehydrogenase kinase) against cancer cells with defects in the electron transport chain has been shown [50]. Also, it was shown that administration of dichloroacetate to mice with inoculated LLC/R9 cells significantly inhibited metastasis without affecting the growth of the primary tumor [51]. A glycolysis inhibitor 2-Deoxy-D-glucose (that possessed neither antitumor nor antimetastatic activity against LLC/R9 in monotherapy in the studied dose) combined with DCA didn't enhance the antimetastatic activity of DCA still, inhibited the growth of the primary tumor.

There is a reason to believe that the antitumor effect (and possibly antimetastatic one) of glycolysis inhibitors in combination with pharmacological agents that can activate OXPHO can also be effective against malignant neoplasms with the normal mitochondrial system.

5. Conclusions

So, our study showed (as far as we know for the first time) the existence of a correlation between the metastatic potential of cells (determined *in vivo*) and their sensitivity to anoikis (assessed *in vitro*): the higher was the metastatic potential of cells, the higher was the degree of their resistance to anoikis. The transition of cells of both LLC variants to anchorage-independent growth was characterized by a decrease in survival, a slowdown in growth rates and was accompanied by an increase in intracellular ROS levels and glucose consumption rates, which was much more pronounced in low-metastatic LLC/R9 cells.

Intracellular metabolism of highly metastatic LLC cells, possessing the normal mitochondrial system, ensured a progressive decrease in both intracellular ROS levels and their apoptotic death, promoting survival during the transition to anchorage-independent growth.

In contrast to LLC, a significant increase in the rate of glucose consumption by the low-metastatic LLC/R9 cells did not lead to a decrease in the extremely high (compared to LLC) levels of ROS (either due to a defective mitochondrial system of these cells or, possibly, malfunctioning of the antioxidant system), which caused lower survival under conditions of anchorage-independent growth and, as a result, greater sensitivity to anoikis.

The correlations identified in the study did not provide a direct proof of a cause-and-effect relationship between the metastatic potential of the cells determined *in vivo* and parameters of glucose metabolism and cell survival investigated *in vitro*. The effect of glycolysis inhibitors on cancer cell sensitivity to anoikis and their metastatic potential should be studied to confirm the reliability of the identified correlations.

Funding

This work was supported by the National Research Foundation of Ukraine (2021.01/0229) and by the National Academy of Sciences of Ukraine (0121U113838).

Ethics approval and consent to participate

In vivo study was approved by the Ethics Committee of the R.E.Kavetsky Institute of Experimental Pathology, Oncology and Radiobiology of the National Academy of Science of Ukraine (protocol No. 4 dated October 21, 2021).

Data availability

The original research data is available for free access on the cloud-based communal repository Mendeley Data, under the title D-23-53909, with the https://doi.org/10.17632/s82r3sc6s5.

CRediT authorship contribution statement

G.I. Solyanik: Writing – original draft, Supervision, Project administration, Formal analysis, Data curation, Conceptualization. **D.**

L. Kolesnik: Software, Methodology, Investigation. **I.V. Prokhorova:** Writing – review & editing, Visualization, Validation. **O.V. Yurchenko:** Visualization, Methodology, Investigation, Formal analysis. **O.N. Pyaskovskaya:** Methodology, Investigation, Data curation.

Declaration of competing interest

The authors declare that they have no known competing financial interests or personal relationships that could have appeared to influence the work reported in this paper.

Acknowledgments

All authors express their sincere gratitude to the Armed Forces of Ukraine, which ensured our safety and made it possible to complete research in 2023, which was mainly done in 2021.

Appendix A. Supplementary data

Supplementary data to this article can be found online at https://doi.org/10.1016/j.heliyon.2024.e32626.

References

[1] C.L. Chaffer, R.A. Weinberg, A perspective on cancer cell metastasis, Science 331 (6024) (2011) 1559–1564, https://doi.org/10.1126/science.1203543.
[2] M. Aleckovic, S.S. McAllister, K. Polyak, Metastasis as a systemic disease: molecular insights and clinical implications, Biochim. Biophys. Acta Rev. Canc 1872 (2019) 89–102, https://doi.org/10.1016/j.bbcan.2019.06.002.
[3] H. Yang, Y.H. Kuo, Z.I. Smith, J. Spangler, Targeting cancer metastasis with antibody therapeutics, Wiley Interdiscip. Rev. Nanomed. Nanobiotechnol. 13 (4) (2021) e1698, https://doi.org/10.1002/wnan.1698.
[4] M.M. González-Ballesteros, C. Mejía, L. Ruiz-Azuara, Metallodrugs: an approach against invasion and metastasis in cancer treatment, FEBS Open Bio 12 (5) (2022) 880–899, https://doi.org/10.1002/2211-5463.13381.
[5] R.L. Anderson, T. Balasas, J. Callaghan, et al., Cancer research UK and cancer therapeutics CRC Australia metastasis working group. A framework for the development of effective anti-metastatic agents, Nat. Rev. Clin. Oncol. 16 (3) (2019) 185–204, https://doi.org/10.1038/s41571-018-0134-8.
[6] Z. Deng, H. Wang, J. Liu, et al., Comprehensive understanding of anchorage-independent survival and its implication in cancer metastasis, Cell Death Dis. 12 (7) (2021) 629, https://doi.org/10.1038/s41419-021-03890-7.
[7] P. Paoli, E. Giannoni, P. Chiarugi, Anoikis molecular pathways and its role in cancer progression, Biochim. Biophys. Acta 1833 (12) (2013) 3481–3498, https://doi.org/10.1016/j.bbamcr.2013.06.026.
[8] F.O. Adeshakin, A.O. Adeshakin, L.O. Afolabi, et al., Mechanisms for modulating anoikis resistance in cancer and the relevance of metabolic reprogramming, Front. Oncol. 11 (2021) 626577, https://doi.org/10.3389/fonc.2021.626577.
[9] H. Dianat-Moghadam, M. Azizi, S.Z. Eslami, et al., The role of circulating tumor cells in the metastatic cascade: biology, technical challenges, and clinical relevance, Cancers 12 (4) (2020) 867, https://doi.org/10.3390/cancers12040867.
[10] J.D. Hayes, A.T. Dinkova-Kostova, K.D. Tew, Oxidative stress in cancer, Cancer Cell 38 (2020) 167–197, https://doi.org/10.1016/j.ccell.2020.06.001.
[11] M. Benzarti, C. Delbrouck, L. Neises, et al., Metabolic potential of cancer cells in context of the metastatic cascade, Cells 9 (9) (2020) 2035, https://doi.org/10.3390/cells9092035.
[12] G. Bergers, S.M. Fendt, The metabolism of cancer cells during metastasis, Nat. Rev. Cancer 21 (3) (2021) 162–180, https://doi.org/10.1038/s41568-020-00320-2.
[13] G. Kroemer, J. Pouyssegur, Tumor cell metabolism: cancer's Achilles' heel, Cancer Cell 13 (6) (2008) 472–482, https://doi.org/10.1016/j.ccr.2008.05.005.
[14] M.V. Liberti, J.W. Locasale, The Warburg effect: how does it benefit cancer cells? Trends Biochem. Sci. 41 (3) (2016) 211–218, https://doi.org/10.1016/j.tibs.2015.12.001.
[15] J. Lu, M. Tan, Q. Cai, The Warburg effect in tumor progression: mitochondrial oxidative metabolism as an anti-metastasis mechanism, Cancer Lett. 35 (2 Pt A) (2015) 156–164, https://doi.org/10.1016/j.canlet.2014.04.001.
[16] J. Lu, The Warburg metabolism fuels tumor metastasis, Cancer Metastasis Rev. 38 (1–2) (2019) 157–164, https://doi.org/10.1007/s10555-019-09794-5.
[17] O.G. Fedorchuk, O.M. Pyaskovskaya, L.M. Skivka, et al., Paraneoplastic syndrome in mice bearing high-angiogenic variant of Lewis lung carcinoma: relations with tumor derived VEGF, Cytokine 57 (1) (2012) 81–88, https://doi.org/10.1016/j.cyto.2011.10.022.
[18] M. Lee, A. Jo, S. Lee, et al., 3-bromopyruvate and buthionine sulfoximine effectively kill anoikis-resistant hepatocellular carcinoma cells, PLoS One 12 (3) (2017) e0174271, https://doi.org/10.1371/journal.pone.0174271.
[19] I. Nicoletti, G. Migliorati, M.C. Pagliacci, et al., A rapid and simple method for measuring thymocyte apoptosis by propidium iodide staining and flow cytometry, J. Immunol. Methods 139 (2) (1991) 271–279, https://doi.org/10.1016/0022-1759(91)90198-o.
[20] H. Wang, J.A. Joseph, Quantifying cellular oxidative stress by dichlorofluorescein assay using microplate reader, Free Radic. Biol. Med. 27 (5–6) (1999) 612–616, https://doi.org/10.1016/s0891-5849(99)00107-0.
[21] S. Yazdanparast, A. Benvidi, S. Abbasi, S.K. Sabbagh, Monitoring the mechanism of anti-cancer agents to inhibit colorectal cancer cell proliferation: enzymatic biosensing of glucose combined with molecular docking, Enzym. Microb. Technol. 148 (2011) 109804, https://doi.org/10.1016/j.enzmictec.2021.109804.
[22] M.S. Lahijani, S.E. Nojooshi, S.F. Siadat, Light and electron microscope studies of effects of 50 Hz electromagnetic fields on preincubated chick embryo, Electromagn. Biol. Med. 26 (2) (2007) 83–98, https://doi.org/10.1080/15368370601185888.
[23] G.C. Yang, T. Scognamiglio, W.I. Kuhel, Fine-needle aspiration of mucin-producing thyroid tumors, Acta Cytol. 55 (6) (2011) 549–555, https://doi.org/10.1159/000333228.
[24] Y. Dai, X. Zhang, Y. Ou, et al., Anoikis resistance – protagonists of breast cancer cells survive and metastasize after ECM detachment, Cell Commun. Signal. 21 (1) (2023) 190, https://doi.org/10.1186/s12964-023-01183-4.
[25] C.D. Simpson, K. Anyiwe, A.D. Schimmer, Anoikis resistance and tumor metastasis, Cancer Lett. 272 (2) (2008) 177–185, https://doi.org/10.1016/j.canlet.2008.05.029.
[26] S.U. Khan, K. Fatima, F. Malik, Understanding the cell survival mechanism of anoikis-resistant cancer cells during different steps of metastasis, Clin. Exp. Metastasis 39 (5) (2022) 715–726, https://doi.org/10.1007/s10585-022-10172-9.
[27] S. Vanharanta, J. Massague, Origins of metastatic traits, Cancer Cell 24 (4) (2013) 410–421, https://doi.org/10.1016/j.ccr.2013.09.007.
[28] Y. Suhail, M.P. Cain, K. Vanaja, et al., Systems biology of cancer metastasis, Cell Syst 9 (2) (2019) 109–127, https://doi.org/10.1016/j.cels.2019.07.003.

[29] M. Benzarti, C. Delbrouck, L. Neises, et al., Metabolic potential of cancer cells in context of the metastatic cascade, Cells 9 (9) (2020) 2035, https://doi.org/10.3390/cells9092035.
[30] S.U. Khan, K. Fatima, F. Malik, Understanding the cell survival mechanism of anoikis-resistant cancer cells during different steps of metastasis, Clin. Exp. Metastasis 39 (5) (2022) 715–726, https://doi.org/10.1007/s10585-022-10172-9.
[31] L.K. Boroughs, R.J. DeBerardinis, Metabolic pathways promoting cancer cell survival and growth, Nat. Cell Biol. 17 (4) (2015) 351–359, https://doi.org/10.1038/ncb3124.
[32] T. Schild, V. Low, J. Blenis, et al., Unique metabolic adaptations dictate distal organ-specific metastatic colonization, Cancer Cell 33 (3) (2018) 347–354, https://doi.org/10.1016/j.ccell.2018.02.001.
[33] K. Ohshima, E. Morii, Metabolic reprogramming of cancer cells during tumor progression and mtastasis, Metabolites 11 (1) (2021) 28, https://doi.org/10.3390/metabo11010028.
[34] B. Faubert, A. Solmonson, R.J. DeBerardinis, Metabolic reprogramming and cancer progression, Science 368 (6487) (2020) eaaw5473, https://doi.org/10.1126/science.aaw5473.
[35] P.P. Hsu, D.M. Sabatini, Cancer cell metabolism: Warburg and beyond, Cell 134 (5) (2008) 703–707, https://doi.org/10.1016/j.cell.2008.08.021.
[36] W.H. Koppenol, P.L. Bounds, C.V. Dang, Otto Warburg's contributions to current concepts of cancer metabolism, Nat. Rev. Cancer 11 (5) (2011) 325–337, https://doi.org/10.1038/nrc3038.
[37] A. Mohamed, X. Deng, F.R. Khuri, et al., Altered glutamine metabolism and therapeutic opportunities for lung cancer, Clin. Lung Cancer 15 (1) (2014) 7–15, https://doi.org/10.1016/j.cllc.2013.09.001.
[38] K. Vanhove, E. Derveaux, G.J. Graulus, et al., Glutamine addiction and therapeutic strategies in lung cancer, Int. J. Mol. Sci. 20 (2) (2019) 252, https://doi.org/10.3390/ijms20020252.
[39] J. Zhang, N.N. Pavlova, C.B. Thompson, Cancer cell metabolism: the essential role of the nonessential amino acid, glutamine, EMBO J. 36 (10) (2017) 1302–1315, https://doi.org/10.15252/embj.201696151.
[40] H. Endo, S. Owada, Y. Inagaki, et al., Metabolic reprogramming sustains cancer cell survival following extracellular matrix detachment, Redox Biol. 36 (2020) 101643, https://doi.org/10.1016/j.redox.2020.101643.
[41] T. Ariizumi, A. Ogose, H. Kawashima, et al., Multinucleation followed by an a cytokinetic cell division in myxofibrosarcoma with giant cell proliferation, J. Exp. Clin. Cancer Res. 28 (1) (2009) 44, https://doi.org/10.1186/1756-9966-28-44.
[42] S. Shadfar, S. Parakh, M.S. Jamali, et al., Redox dysregulation as a driver for DNA damage and its relationship to neurodegenerative diseases, Transl. Neurodegener. 12 (1) (2023) 18, https://doi.org/10.1186/s40035-023-00350-4.
[43] Y. Liu, Y. Sun, Y. Guo, et al., An overview: the diversified role of mitochondria in cancer metabolism, Int. J. Biol. Sci. 19 (3) (2023) 897–915, https://doi.org/10.7150/ijbs.81609.
[44] S. Arfin, N.K. Jha, S.K. Jha, et al., Oxidative stress in cancer cell metabolism, Antioxidants 10 (5) (2021) 642, https://doi.org/10.3390/antiox10050642.
[45] Y. Wang, H.H. Liu, Y.T. Cao, et al., The role of mitochondrial dynamics and mitophagy in carcinogenesis, metastasis and therapy, Front. Cell Dev. Biol. 8 (2020) 413, https://doi.org/10.3389/fcell.2020.00413.
[46] O. Warburg, On the origin of cancer cells, Science 123 (1956) 309–314, https://doi.org/10.1126/science.123.3191.309.
[47] W.H. Koppenol, P.L. Bounds, C.V. Dang, Otto Warburg's contributions to current concepts of cancer metabolism, Nat. Rev. Cancer 11 (2011) 325–337, https://doi.org/10.1038/nrc3038.
[48] Y. Yang, S. Karakhanova, W. Hartwig, et al., Mitochondria and mitochondrial ROS in cancer: novel targets for anticancer therapy, J. Cell. Physiol. 231 (12) (2016) 2570–2581, https://doi.org/10.1002/jcp.25349.
[49] C. Musicco, A. Signorile, V. Pesce, et al., Mitochondria deregulations in cancer offer several potential targets of therapeutic interventions, Int. J. Mol. Sci. 24 (13) (2023) 10420, https://doi.org/10.3390/ijms241310420.
[50] L.H. Stockwin, S.X. Yu, S. Borgel, et al., Sodium dichloroacetate selectively targets cells with defects in the mitochondrial ETC, Int. J. Cancer 127 (11) (2010) 2510–2519, https://doi.org/10.1002/ijc.25499.
[51] O.N. Pyaskovskaya, D.L. Kolesnik, A.G. Fedorchuk, et al., 2-Deoxy-D-glucose enhances dichloroacetate antitumor action against Lewis lung carcinoma, Exp. Oncol. 38 (3) (2016) 176–180.